J Therm Anal Calorim (2017) 129:821–832
DOI 10.1007/s10973-017-6190-y

Structural transformation, thermal endurance, and identification of evolved gases during heat treatment processes of carbon fiber polymer precursors focusing on the stereoregularity

G. Santhana Krishnan[1] · N. Murali[1] · A. Jafar Ahamed[2]

Received: 29 March 2016 / Accepted: 11 February 2017 / Published online: 1 March 2017

Abstract Structural transformations of polyacrylonitrile microstructure with varying degrees of stereoregularity during the thermal-oxidative degradation and pyrolysis reactions were investigated employing coupled thermal techniques namely pyrolysis–gas chromatography–mass spectrometry, evolved gas analysis–mass spectrometry, and thermal gravimetric analyzer-FT infrared spectrometry (TG-FTIR) in the temperature range of 200–600 °C. More number of intense peaks with large ionic abundances in the thermal curves and pyrograms indicate that atactic-rich polyacrylonitrile copolymers undergo thermal cleavage, fragmentation and cyclization reactions more readily than isotactic polyacrylonitrile. The mass loss accompanying the thermal reactions was accounted for the evolution of hydrogen cyanide, ammonia, and homologous of alkyl nitrile having molar mass between 47 and 224 *m*/*z*; their most probable structures were identified. Thermal analysis results confirm that nitrile cyclization reactions proceed preferentially at isotactic triads leading to a steady and stable thermal-oxidative degradation reactions as compared to atactic-rich polyacrylonitrile. The simultaneous TG-FTIR results of evolved gas analysis also validate the pyrolysis experiments.

✉ G. Santhana Krishnan
santhana@nal.res.in

[1] Materials Science Division, CSIR-National Aerospace Laboratories, Bangalore 560017, India

[2] Department of Chemistry, Jamal Mohammed College (Autonomous), Bharathidasan University, Tiruchirappalli, India

Keywords Triad tacticity content · Average molecular masses · Coupled thermal techniques · Fragmentation and evolved gases

Introduction

Carbon fibers (CF) make up a significant volume fraction of modern structural airframe materials, they provide significant structural strength, stiffness gains and are lightweight when embedded into a suitable polymer resin matrices [1–5]. Carbon fibers are fibrous carbon materials with a micrographite crystal structure, classified by the source materials such as rayon, polyacrylonitrile (PAN), pitch and lignin [6–8]. In general, carbon fibers have superior mechanical properties, which include high specific strength and specific modulus, as well as characteristics such as low density, low thermal expansion, and high corrosion resistance. Polyacrylonitrile-based polymers (PAC) are an important class of precursors for high value carbon-based materials, such as carbon fiber with high mechanical, thermal resistance, and mesoporous carbon for use in photo-electronic devices [9]. In recent years, polyacrylonitrile-based polymers have emerged as the most preferred polymer precursors for high-tensile-grade carbon fibers due to their high carbon yield on carbonization above 1000 °C, facile polymerization with other comonomers. Almost more than ninety percent of commercially available carbon fibers are derived from PAC [10]. High-tensile carbon fibers enable the fabrication of lightweight, durable, and cryogenic high-pressure vessels for storage of compressed hydrogen gases in space launch vehicles [11, 12]. This trend requires a higher level of understanding and improvements of physical characteristics in the carbon fiber polymer precursors. The industrial production of

high-tensile-grade carbon fiber includes polymer synthesis, fiber spinning, thermal-oxidative stabilization, and carbonization [13]. One of the critical stages in the carbon fiber fabrication process is the heat treatment process, including thermal stabilization of acrylic precursors through flame-resisting treatment and primary carbonization. During this process, PAC precursors are subjected to a controlled heat treatment in air at temperature in the range 200–600 °C. In the carbonization process, the stabilized fibers are further heated at the temperatures in the range 300–2800 °C.

The thermal-oxidative stabilization and primary carbonization are considered very significant as the formation of a thermally inert, cyclized and aromatized structure takes place during this process, which are determinant in deciding tensile properties in the downstream processes of carbonization and graphitization. In particular, stabilization process is conducted in prohibitively slow rates; however, in order to improve the industrial production rate of carbon fibers, the optimization of stabilization step is very much desired. Technically, carbon fiber fabrication is a process of controlled and constructive pyrolysis of PAC precursors into a less defective carbonaceous structure in a linear form. Usually, heat treatment processes are accompanied by the evolution of gases in substantial quantities consisting of oxides of carbon (CO, CO2), hydrogen cyanide (HCN), small molecules of alkyl nitrile compounds (RCN) [14–16]. The oxidative cyclization and aromatization are not simple thermal reactions, but are influenced by various factors such as polymer structure, linear density (dtex), chemical composition of the precursor; specifically, comonomers influence the thermal reactions significantly [17–19]. As a function of polymerization techniques, structurally PAN copolymers are synthesized in three different stereo-structures, viz. isotactic, atactic, and syndiotactic. The stereo-structure or structural regularity of the pendant groups in linear polymers is quantified in terms of tacticity contents, more precisely triad tacticity. It has been reported that the microstructure of polymer main chain as described in terms of stereoregularity can influence the reaction temperature and reaction rate of thermally induced cyclization reactions [20]. In our previous article, the distinct thermal degradation behavior of stereoregular polyacrylonitrile due to the higher isotactic triad content was investigated using conventional thermal analytical techniques (DSC, TG) and stereoregular PAN was found to have more thermal stability, comparatively [21]. The tensile properties of CFs are highly dependent on the process parameters maintained during CF manufacture, especially tensile strength of filaments which are very sensitive to surface defects and internal voids [22]. The formation of defects and voids is mainly due to the evolution of gaseous molecules and certain molecular defects from the CF precursors [23].

Minagawa et al. [24] applied pyrolysis–gas chromatography technique to study the thermal degradation behavior of CF polymer precursors under rapid pyrolysis conditions and established the secondary thermal degradation, fragmentation reactions of polyacrylonitrile during the pyrolysis. Fitzer et al. [15] established the dependence of tensile strength of carbon fiber on the quantity of evolved gas released. Tensile properties of carbon fibers are highly dependent on the heat treatment temperatures that range from 200 to 3000 °C, shrinkage stresses developed in the filaments, and release of various molecular species as evolved gases [25–27]. Therefore, the identification of evolved gaseous molecules during carbonization process will certainly improve the general understanding of defects, microvoids formation, and pattern of decomposition and structural formation of carbon fiber when it is subjected to a severe thermal treatment. Conventional thermal techniques, viz. thermal gravimetric analysis (TG), differential scanning calorimetry (DSC), and differential thermal analysis (DTA), are commonly used in the thermal studies of carbon fiber polymers precursors; however, they are not capable of acquiring qualitative and quantitative structural transformations during the thermal stabilization, cyclization, and carbonization processes. This article investigates the influence of microstructure, in terms of the triad tacticity content of cyano functionalities of poly(acrylonitrile) on the structural transformation, thermal stability, and identification of evolved gaseous species in heat treatment processes applying coupled thermal analytical techniques. The detailed thermal investigations were performed applying hyphenated thermal techniques such as pyrolysis–gas chromatography–mass spectrometry (Py–GC–MS), evolved gas analysis–mass spectrometry (EGA–MS), and TG-FTIR, in addition to the confirmation of stereochemical configuration of PAN polymers applying nuclear magnetic resonance techniques.

Experimental

Materials

Synthesis grade acrylonitrile (AN) [Aldrich Co., 99%] was used in the polymer synthesis. Acrylonitrile was washed with sodium hydroxide solution of lower concentration 0.5 mass% and distilled at its boiling range just before polymerization to remove the inhibitor content. The hexagonal crystalline metal salts (nickel chloride or magnesium chloride) [Sigma-Aldrich Co. Ltd.,] were used as a template compound. Commercially available α, α

azoisobutyronitrile (AIBN) [Wako Pure Chemical Industries, Ltd.] was used as initiator after crystallization in methanol. Analytical grade dimethylformamide (DMF) [Sigma-Aldrich Co. Ltd.] was used for the measurements of polymer solution properties.

Synthesis of isotactic poly(acrylonitrile) (I-PAN) and atactic poly(acrylonitrile) (A-PAN)

The polymerization was carried out in a 500-mL three-necked round bottom flask, equipped with mechanical stirrer and a reflux condenser. The flask was bubbled with ultra pure N_2 gas for 30–60 min at a flow rate of 30 mL min^{-1} to ensure an oxygen-free atmosphere. The template compounds used in this polymer synthesis are a hexagonal crystalline metal salt ($NiCl_2$ or $MgCl_2$). The polymerization procedures as described in our previous work were followed for the synthesis of I-PAN and A-PAN [28]. The resulting polymer was filtered and washed with methanol and deionized water to dried at 60 °C under vacuum to a constant mass.

Characterization

Molecular characterizations

Average molecular mass determinations Size exclusion chromatography–low-angle laser light scattering (SEC-LALLS).

The chromatography parameters [molecular mass distribution and polydispersity index (M_w/M_n)] were determined by SEC-LALLS instrument of Malvern Viscotek TDA 305 (Triple Detector Array). The carrier solvent was DMF containing 0.05 M lithium bromide with a flow a rate of 1 mL min^{-1} and injection volume of 100 µL at 50. A concentration of $\sim$4.0 mg mL^{-1} was maintained in all samples. SEC-LALLS instrument was used as a detector at a fixed wavelength of 633 nm. Before the injection, samples were filtered through a PTFE membrane with 0.2 mm pore. The molecular mass parameters were computed using SEC-LALLS data processing system. A set of polymethyl methacrylate standards of narrow molecular mass distribution (PolyCALTM, Viscotek, US) of molecular mass 2.0×10^4–4.51×10^5 g mol_{-1} was used to calibrate the SEC-LALLS instrument.

Solution viscometry

Measurements of viscometric parameters were taken with an accuracy of 1/100 s in dimethylformamide at 30 ± 0.02 °C in a constant temperature viscometer bath, with the use of an Ubbelohde-type capillary viscometer (Rheotek Co., UK). The trend in the viscosity-average molecular masses from time to time was determined using the following empirical intrinsic viscosity-molecular eight relationships as in Eqs. 1–3 [29, 30]. The values of k and α are 2.53×10^{-4} and 0.72, respectively.

$$\eta_{sp} = \eta_{so\,ln} - \eta_{solv}/\eta_{solv} = \eta_{rel} - 1 \quad (1)$$

$$[\eta] = \left\{\left(1.44 * \eta_{sp} + 1\right)\right\}^{1/2} - 1/0.36 \quad (2)$$

$$[n] = k[M_v]^{\alpha} \quad (3)$$

^{13}C NMR

The ^{13}C NMR (Bruker AMX-400) spectra of the polymers were recorded in DMSO using tetramethylsilane (TMS) as an internal standard. Samples were concentrated in dimethyl sulfoxide about 5% (w/w) for ^{13}C NMR by using a 5 mm NMR tube at room temperature. ^{13}C NMR spectra were acquired using 24,996 data points, spectral width 22 kHz, broadening 3 Hz, pulse delay 2 s, pulse width 90°, and 1024 scans. Nuclear overhauser effect (NOE) was suppressed by gating the decouple sequence. Heteronuclear multiple quantum coherence (HMQC) was performed by using the standard Bruker pulse sequence with a pulse program. The spectrum was obtained with 256 increments in the F1 dimension and 1024 data points in the F2 dimension, with 200 scans and relaxation delay 1.5.

Thermal characterizations using hyphenated thermal techniques

Pyrolysis–gas chromatography–mass spectrometry

The configuration of Py–GC/MS as developed by Chuichi Watanabe et al. [31] was employed for the evaluation of thermal-oxidative degradation of the polymer samples under investigation. A small amount of powdery sample was taken in a deactivated stainless steel sample cup and then mounted into the pyrolyzer. The multifunctional pyrolyzer EGA/PY-3030D model (Frontier Laboratories, Japan) which is capable of heating a sample from near room temperature to 800 °C at a desired rate between 1 and 40 °C min_{-1} was used to heat up the sample. Evolved gases released during the heat-up was directly separated and analyzed by the GC/MS (GC–Ms-QP2010, GC–MS ITFtemp.280 °C, *m/z*: 27-600 IS temp.: 200). The remaining residue in the sample cup was analyzed on the same system by EGA–MS single-shot analysis. In the GC–MS system, the evolved gas mixture was continuously introduced to the sample loops and separated into the constituents by the chromatographic column. The carrier gas is removed by the separator, and only the components to be determined are introduced directly into the mass spectrometer to obtain mass spectrum. The pattern

of thermal degradation and the structural changes accompanying degradation was estimated from the obtained thermal curves and pyrograms.

TG-Fourier transform Infrared spectrometer

The analysis of evolved gases from polymer samples was carried out using a hyphenated system of the TG 4000/Pyris 6 (Perkin Elmer) coupled to a frontier FTIR spectrometer. The typical analysis conditions are as follows: wave number, 400–4000 cm^{-1}; resolution, 2 cm^{-1}; purging gas, N2 (flow rate, 20 mL min^{-1}); heating rate, 20 °C; temperature range 40–650 °C; specimen mass, 12.00 mg.

Results and discussion

Synthesis and molecular and structural characteristics

The synthetic pathways employed for the gram-scale preparation of both isotactic (I-PAC) and atactic (A-PAC) polyacrylonitrile copolymers are represented in the reaction Scheme 1. Polyacrylonitrile copolymer with stereoregularity defined in terms of triad tacticity of cyanide functional groups with isotactic triads in excess of 50 mass%, and atactic triads over 45 mass% were synthesized using solid-state polymerization assisted by templates and solution polymerization in mixed solvents, respectively.

The percentage conversion of monomers to polymer in both polymerization processes was found to be around 75 mass% through analytical gravimetry. The progress of the polymerization reaction has been monitored by measuring the specific viscosity of the reaction mixture.

Where $k(3.35 \times 10^{-4})$ and α (0.72) are Mark–Houwink parameter which depends on the kind of solvents used for the solution viscometry measurements. The concentration of the polymers in the solution was varied from 0 to 2.0 g dL^{-1}. The average molecular masses (M_w, M_n) and the molecular mass distribution (M_w,/M_n) of polymers synthesized in this study were estimated using size exclusion chromatography with low-angle laser light scattering detector (LALLS) and solution viscometry which are listed in Table 1. The viscosity-average molecular mass (M_v), number average molecular mass (M_n), and mass average molecular mass of the polymer samples used in this investigation are 1.69–2.06 $\times$ 10^5, 10.7–2.13 $\times$ 10^4, and 1.72–2.13 $\times$ 10^5, respectively.

Figure 1 shows the ^{13}C-NMR spectra of two different stereoregular polyacrylonitrile samples, viz. I-PAC, and A-PAC. The stereoregularity of substituted vinyl polymers is usually determined in terms of triad tacticity of pendant functionalities. There are three distinct carbon

Scheme 1 Reaction pathways used for synthesis of polyacrylonitrile with different stereo

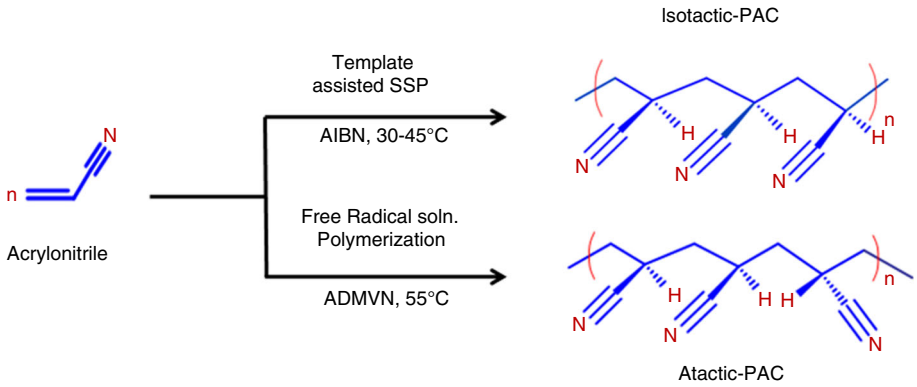

Table 1 Molecular characteristics of polyacrylonitrile copolymers with different stereo-structures

Polymer code	Polymer Compsn.—feed/mol%		Convn./mass%	η_{iv}/dLg^{-1}	$M_v \times 10^{-5}$/Da	$M_w \times 10^{-5}$/Da	$M_n \times 10^{-4}$/Da
	AN	IA					
I-PAC/01	98.5	1.5	74	2.24	2.06	2.13	12.3
I-PAC/02	98.5	1.5	74	2.01	1.76	2.38	10.7
A-PAC/01	98.5	1.5	78	2.08	1.86	1.92	11.1
A-PAC/02	98.5	1.5	74	1.94	1.69	1.72	12.8

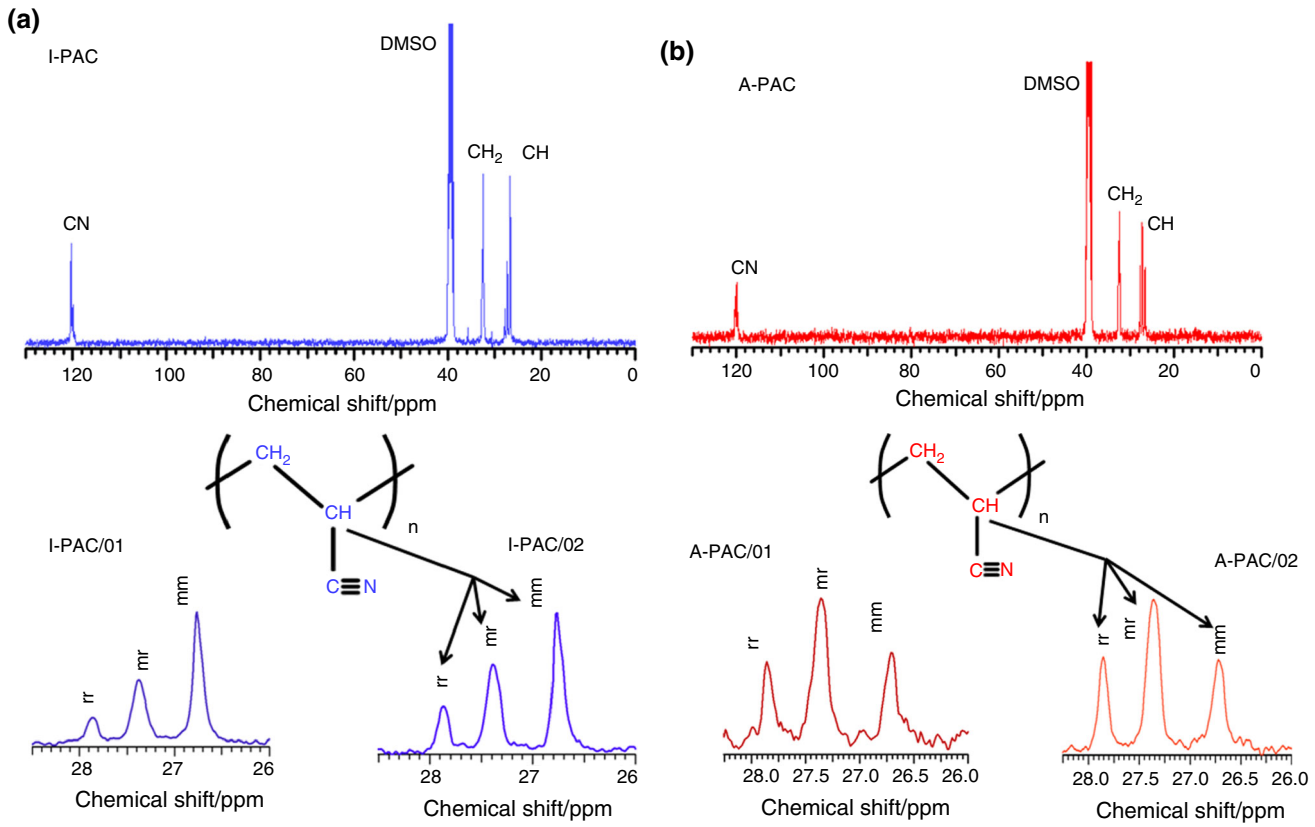

Fig. 1 ^{13}C NMR spectra of two kinds of PAC sample: **a** solid-state polymerization through template (I-PAC); **b** free radical solution polymerization (A-PAC)

resonance absorption peaks observed in both polymer samples corresponding to methine (CH,), methylene (CH_2), and cyano-carbon (CN). The chemical shift value at 40 ppm can be assigned to dimethyl sulfoxide solvent. The methine, methylene, and cyano-carbon chemical shift values (δ) as observed in the ^{13}C-NMR are 26.7–27.9, 32–34, and 120.5–121.0 ppm, respectively. The peak shapes and positions of the methine carbon signals (CH) varied significantly. In solid-state polymerization I-PAC01/02 sample, shape of the peak could be easily distinguishable from that of free radical solution polymerization A-PAC01/02 samples due to stereochemical configuration.

The triad tacticities of the polymers prepared were estimated using methine carbon (CH) signals in the region 26.7–27.9 ppm. They consisted of three main peaks, corresponding to three possible steric triad configurations. The peaks at 26.75, 27.3, and 27.86 ppm correspond to isotactic (mm), atactic (mr), and syndiotactic (rr), respectively. The relative intensities of the peaks corresponding to methine carbon were used for determining the triad tacticity of PAC. The extent of isotacticity (mm) of the I-PAC/01 and

Table 2 Triad tacticity contents of polymer samples used in the study

Synthesis method	Polymer sample ID	Specified group	Chemical shift valuesppm			Triad Tacticity Contents/mass%			$4IS/A^2$
			mm	mr	rr	*I*	*A*	*S*	
Solid-state polymerization	I-PAC/01	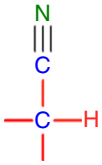	26.77	27.39	27.86	51.4	38.9	14.7	2.629
	I-PAC/02		26.77	27.39	27.85	50.1	35.6	14.3	2.261
Solution polymerization	A-PAC/01		26.72	27.35	27.85	26.7	48.8	24.5	1.098
	A-PAC/02		26.71	27.39	27.86	27.7	47.7	24.6	1.197

02 samples was found to be in the range of 47.6–51.4% (Table 2). The atactic triad contents of the A-PAC01/02 were estimated to be in the range 47.7–48.8%. The Bernoulli statistics is held satisfactorily for the PAC samples as listed in Table 2.

Thermolysis curves and pyrograms of I-PAC and A-PAC and their identification

Figure 2 shows the EGA–MS curves of total ions of the A-PAC (bottom) and I-PAC (top). The A-PAC (bottom) curve displays two peaks with maxima 280 and 440 °C, respectively. There exist two humps at 140 and 360 °C, thereby clearly forming four distinct regions (α, β, δ, and θ) of thermal degradation. From the results of EGA–MS, the pyrolysis temperatures of A-PAC in pyrolysis–GC/MS can be set at 150, 180,260,280,300,320,380,400,450, and 500 °C. However, the EGA thermal curves of the I-PAC

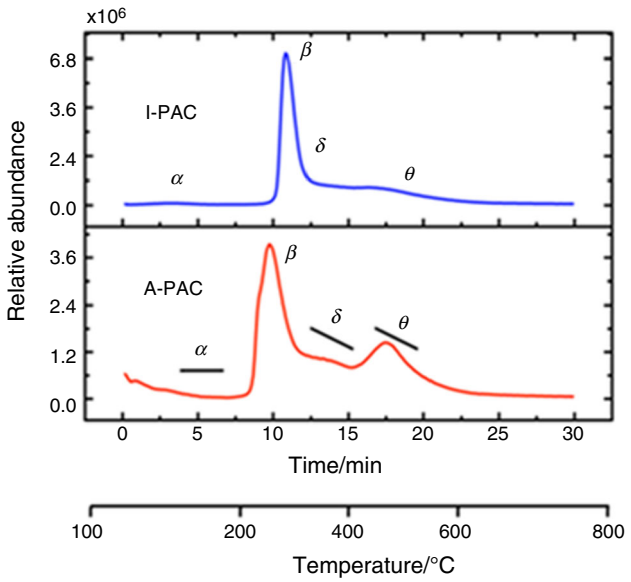

Fig. 2 EGA–MS curves of total ions of the I-PAC, and A-PAC

Table 3 Ionic abundances of peaks corresponding to pyrolysates from Py-GC–MS

m/z value	Molecular formula	Ionic abundance/%	
		A-PAC	I-PAC
28	HCN	70	40
41	CH_3CN,C_3H_5,C_2H_3N	75	50
54	$(C_2H_3CN)H$	70	45
80	$(C_2H_4CN)C_2H_3$	10	30
107	$(C_2H_3CN)_2H$	45	25
121	$(C_2H_3CN)_2CH_3$	25	20

clearly show a peak at 320 °C and shoulders at 380 and 420 °C. Table 3 summarizes the results of identification of the peaks corresponding to the specific mass to charge ratios in the mass spectrum. Most gaseous species evolved are identified as ammonia, hydrogen cyanide, and alkyl nitrile compound

Figure 3 shows typical pyrograms of polyacrylonitrile polymer precursors differing in their microstructure scanned at 100–700 °C. A critical observation at the pyrograms reveals that relative intensity of ionic peak increases as the temperature increases. The major thermal pyrolysates found on the pyrograms are the peaks of low-boiling fragments, acrylonitrile (AN) monomers (A, MA), dimer (AA′, AA_1–AA_3), trimers (AAA1–AAA_4), and tetramers (T_1–T_3) reflecting the AN sequences in the polymer chain. Major peaks are formed mainly due to the thermal scission reaction along the original polymer chain. The ionic abundance observed in the pyrograms corresponding to the relative intensity of gaseous pyrolysates is generally higher for A-PAC, i.e., in the order of 7.4×10^5 as compared to 6.9×10^5 of I-PAC. The presence of relatively more number and high intense peaks in case of A-PAC suggests higher and abrupt release of gaseous pyrolysates during thermal degradation.

Table 4 presents an approximate assignment of peaks corresponding to the various homologous of linear alkyl nitriles (dimer, trimer, and tetramers) as observed pyrograms shown in Fig. 3. The retention index values of eluting gaseous species related respective peaks were estimated by comparing their retention characteristics with those of the closest eluting component in the retention index standards analyzed under similar experimental conditions. Generally, the retention values are highly indicative of the molecular size and masses of the eluting components in pyrolysis reactions. As expected the retention indices increase from 470 to 2294 as the temperature increases from 100 to 700 °C, clearly indicating the higher chain length of alkyl nitriles trimers and tetramers. The relative intensity of the higher homologous is more than lower fragments. Table 5 lists tentative identification of different alkyl nitriles observed in the pyrograms.

Mass spectra of pyrolysates of I-PAC and A-PAC

Figures 4–6 represent the average mass spectra of the molecular species evolved during the pyrolysis experiments in the range 200–600 °C corresponding to the four regions marked in the EGA–MS curves as in Fig. 2. Though there is a distinct quantitative variation of the total ionic abundance of evolved gases in the EGA–MS curves of I-PAC and A-PAC samples, however, qualitatively almost similar molecular species are identified in all four

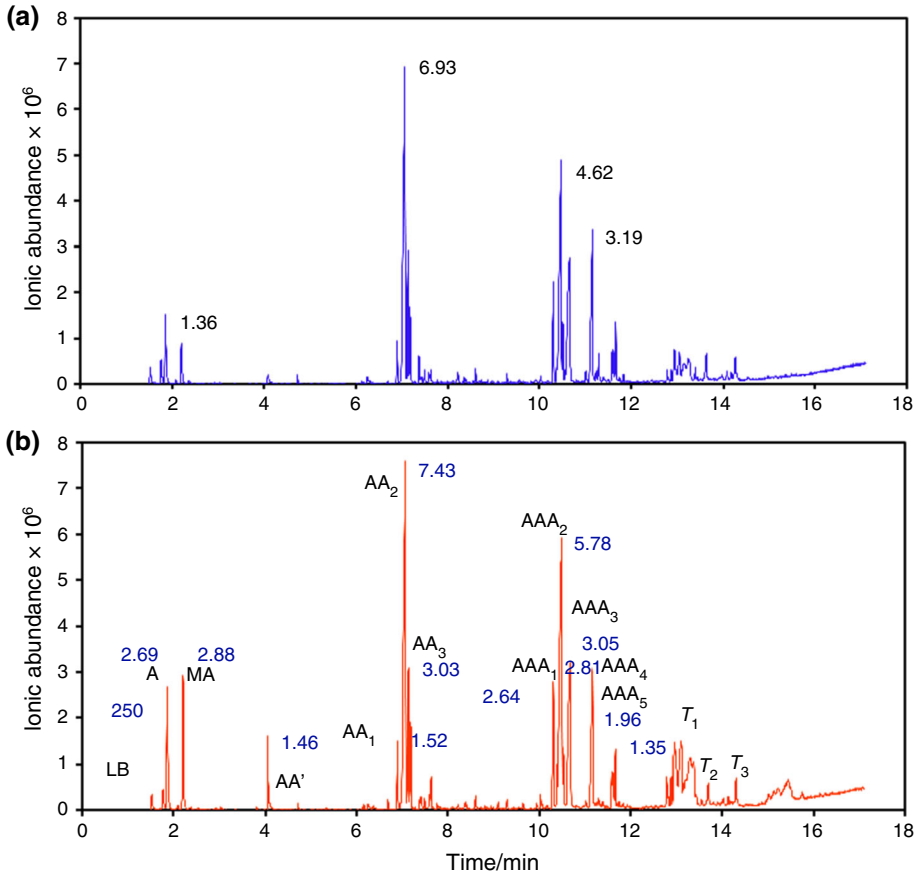

Fig. 3 Pyrograms of polyacrylonitrile sample **a** I-PAC, **b** A-PAC

Table 4 Assignments of peaks of evolved gases in the pyrograms

Peak notation	Assignment of main peaks		Molecular mass/Da	Retention index	Relative intensity/%
LB	Low-boiling point components		–	470	1.4
A	Acrylonitrile	Monomer	53	567	6.2
MA	Methacrylonitrile		67	602	1.1
AA^{I}	C(CN)=C–C–CN	Dimer	92	834	0.9
AA1	C–C(CN)–C=C–CN + C=C(CN)–C–C(CN)		106;120	1045	1.2
AA2	C=C(CN)–C–C–CN + C(CN)–C–C–CN + C=C(CN)–C–C(CN)=C		94;118	1059	64.9
AA3	C–C(CN)–C–C–CN		108	1070	24.4
AAA1	C=C(CN)–C–C–(CN)–C–C–CN	Trimer	159	1513	23.9
AAA2	C–C(CN)–C–C–(CN)–C–C–CN		161	1540	100
AAA3	C(CN)–C–C(CN)–C–C–CN		147	1564	35.9
AAA4	C–C(CN)–C–C–(CN)–C=C–CN		159	1655	39.9
AAA5	$C_9H_9N_3$(isomer of trimer)		159	1743	13.5
T_1	C=C(CN)–C–C–(CN)–C–C–(CN)–C–C–CN	Tetramer	212	2022	23.9
T_2	C=C(CN)–C–C–(CN)–C–C–(CN)–C–C–(CN)=C		224	2155	12.0
T_3	C(CN)–C–C(CN)–C–C–(CN)–C–C–CN		200	2294	9.9

regions marked (α, β, δ, θ) in the mass spectra of both samples. The low-boiling compounds and fragments exhibit both molecular ion peak (M^{+}*) and base peaks, whereas the molecular ion peaks of straight-chain alkyl nitriles are either weak or absent except acetonitrile. The structures of the fragmented molecular species as observed are given in

Table 5 Identification of homologs of alkyl nitriles in the pyrograms

Peak Notation	Assignment of main peaks		Name of the chemical species
LB	Low-boiling point components		–
A	C=C(CN)	Monomer	Acrylonitrile
MA	C–C=C(CN)		Methacrylonitrile
AA′	C(CN)=C–C–CN	Dimer	2-methyl pentanedinitrile
AA1	C–C(CN)–C=C–CN + C=C(CN)–C–C(CN)		2-methylene pentanedinitrile
AA2	C=C(CN)–C–C–CN + C(CN)–C–C–CN + C=C(CN)–C–C(CN)=C		2,4-dimethylpentanedinitrile
AA3	C–C(CN)-C–C–CN		Glutaronitrile
AAA1	C=C(CN)–C–C–(CN)–C–C–CN	Trimer	Hex-5-ene-1,3,5-tricarbonitrile
AAA2	C–C(CN)–C–C–(CN)-–C–C–CN		Hexane-1,3,5-tricarbonitrile
AAA3	C(CN)–C–C(CN)–C–C–CN		Pentane-1,3,5-tricarbonitrile
AAA4	C–C(CN)–C–C–(CN)–C=C–CN		Hex-1-ene-1,3,5-tricarbonitrile
AAA5	$C_9H_9N_3$(isomer of trimer)		Isomer of Hex-1-ene-1,3,5-tricarbonitrile
T_1	C=C(CN)–C–C–(CN)–C–C–(CN)–C–C–CN	Tetramer	Oct-7-ene-1,3,5,7-tetracarbonitrile
T_2	C=C(CN)–C–C–(CN)–C–C–(CN)–C–C–(CN)=C		Nona-1,8-diene-2,4,5,8-tetracarbonitrile
T_3	C(CN)–C–C(CN)–C–C–(CN)–C–C–CN		Heptane-1,3,5,7-tetracarbonitrile

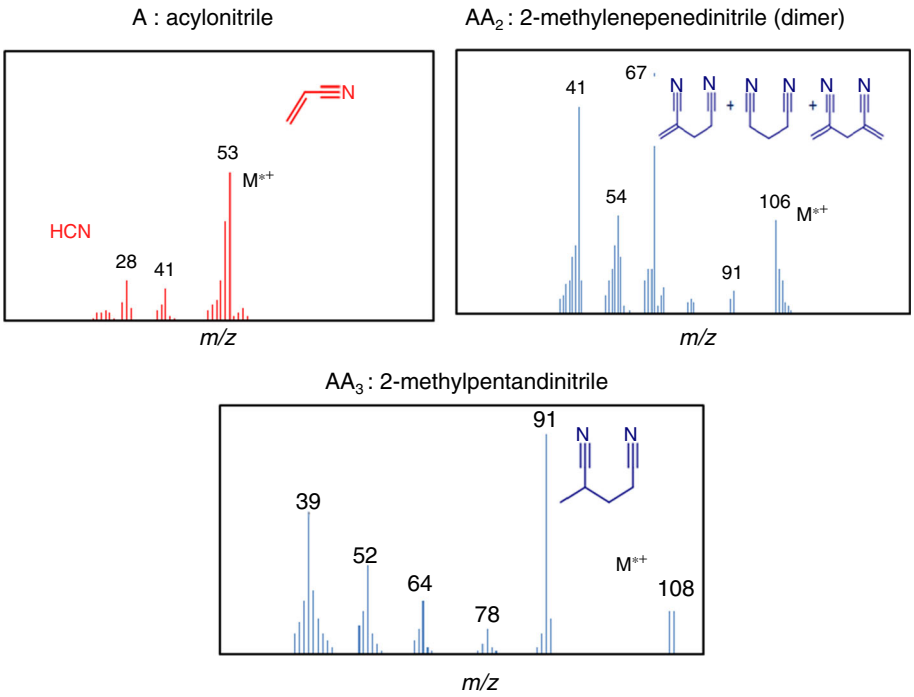

Fig. 4 Mass spectrum of pyrolysis products of I-PAC and A-PAC at 250 °C

their respective mass spectra. The average mass spectra of the low-boiling compounds are depicted in the Fig. 5. The low mass fragments such as acrylonitrile and methacrylonitrile showed the molecular ion peak at 53, 67 *m*/*z* values. Dimers and oligomeric base peaks are observed at ca. 91, and 106 *m*/*z* values, and they can be related to the structural formulas: C–C(CN)-C=C–CN, and/or C=C(CN)–C–C(CN). The other remarkable peak at *m*/*z* 41, 54 are attributed to the formation of CH_3CHCN and CH_2=C=NH, respectively. These structures undergo McLafferty rearrangement to form a methacrylonitrile radical ion peak. The mass spectrum of the decomposition products at 450 °C is shown in Fig. 5, which mainly reflects the release of saturated and unsaturated trimers of acrylonitrile, viz. Hex-5-ene-1,3,5-tricarbonitrile, Hexane-1,3,5-tricarbonitrile, pentane-1,3,5-tricarbonitrile, and Hex-1-ene-1,3,5-tricarbonitrile. Due to high thermal instability at 450 °C, they exhibit weak molecular ion peaks at

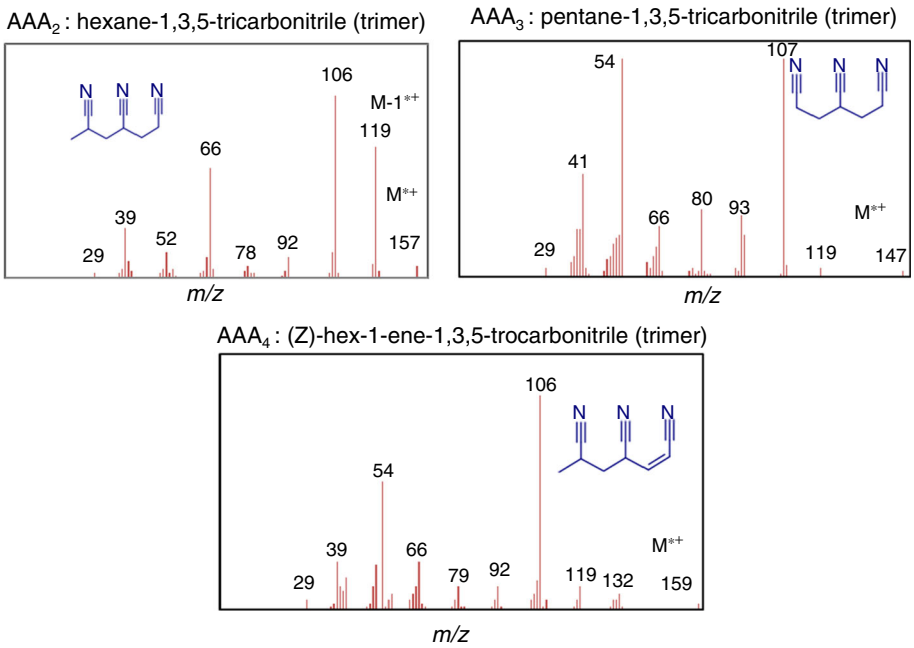

Fig. 5 Mass spectrum of pyrolysis products of I-PAC and A-PAC at 450 °C

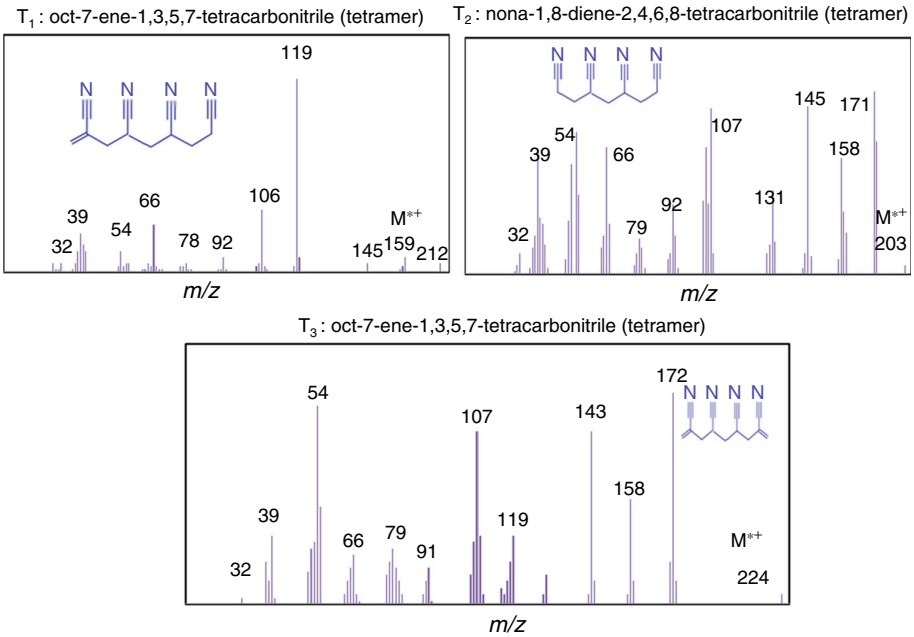

Fig. 6 Mass spectrum of pyrolysis products of I-PAC and A-PAC at 600 °C

147,159 *m/z* values; however, they show a strong molecular ion peaks corresponding to the fragmented dimers as discussed above. Many such peaks observed at 106, 107, and 119 *m/z* are related to dimers, formed by the elimination of methyl and HCN fragments (Fig. 7).

The unsaturated and saturated tetramers of linear alkyl nitriles do not show any strong base peaks, but the peaks at 203,212, and 224 *m/z* are identified as Oct-7-ene-1,3,5,7-tetracarbonitrile, Nona-1,8-diene-2,4,5,8-tetracarbonitrile, and Heptane-1,3,5,7-tetracarbonitrile, respectively. Comparatively, stronger molecular ion peaks related to dimers and trimers are seen at 106, 119, 143, and 158 *m/z* values.

Experimental results presented here suggest that there are two distinct types of thermal reactions responsible for thermal decomposition, pyrolysis and structural transformation of the polyacrylonitrile with varying degrees of stereoregularities. They are thermal fission reactions such as cleavage at α-carbons and side groups of the linear alkyl nitrile and other

thermal rearrangement reactions, viz. generation of unsaturation, cross-linking, and rearrangement leading to more thermally stable structures. General thermal reactions of the polyacrylonitrile leading to gaseous molecular species are represented in Scheme 2.

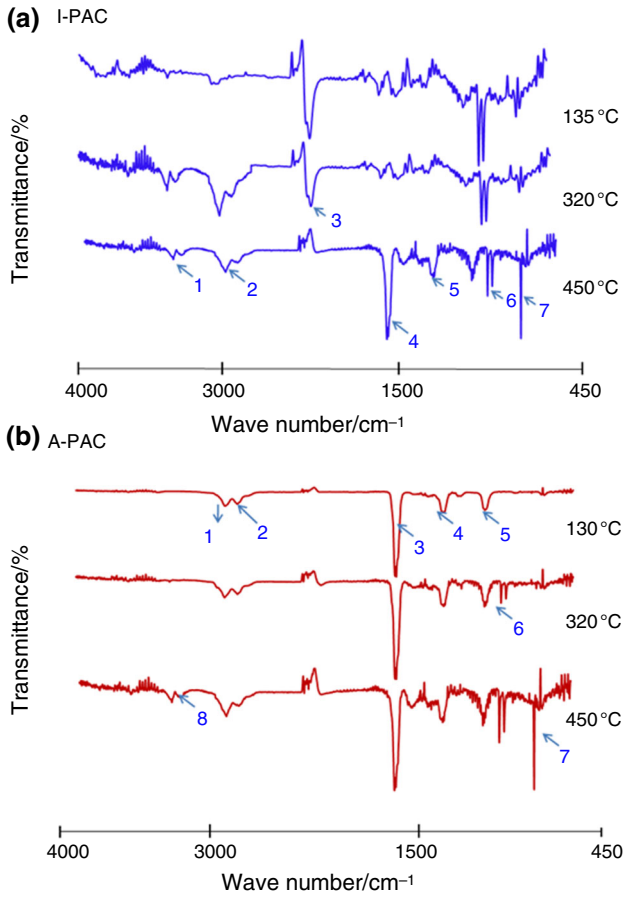

Fig. 7 FTIR spectra of pyrolysis products of **a** I-PAC and **b** A-PAC evolved at different temperatures

FTIR spectra of evolved gases

Figure 6a, b shows the FTIR spectral changes accompanying structural transformations during the pyrolysis reactions of (a) I-PAC and (b) A-PAC at different temperatures, viz. 135, 320, and 450 °C. The distinct difference between the FTIR spectrum of I-PAC and A-PAC FTIR spectrum is very clearly observed. In general, the absorption in the case of I-PAC is less intense to that observed in A-PAC, clearly exhibiting the evolution of more evolved molecular species during thermal processing. This confirms to high thermally labile nature of A-PAC as compared to I-PAC. The peak assignments and identification of the various functional groups present in the evolved molecules at different temperatures are presented in Table 6. It is observed that some spectral absorption peaks become very sharp and stronger, while others disappear in the spectra as the temperature increases. There is strong absorption peak occurs at 2240 cm^{-1} (ν_{C-C-N}) in the temperature range 135–320 °C, and the same peak disappears at 450 °C, suggesting the slow on-set of nitrile cyclization in the case of I-PAC. A new absorption peak appears at 1723 cm^{-1}, assigned to carbonyl stretching functional group ($\nu_{C=O}$) showing the incorporation of oxygen into the cyclic structure of polyacrylonitrile. The absorptions at 2848, 2935 cm^{-1} becomes stronger as the temperature increases from 135 to 450 °C in both cases, clearly indicating the completion of cyclization reaction of the cyano groups. Many strong peaks appearing around 967, 974 cm^{-1} at 450 °C can be assigned to bending frequencies of –NH groups confirming the release of ammonia gas.

Scheme 2 Pyrolysis reactions leading to the formation of several molecular species accounting for peaks observed in the mass spectra of I-PAC and A-PA

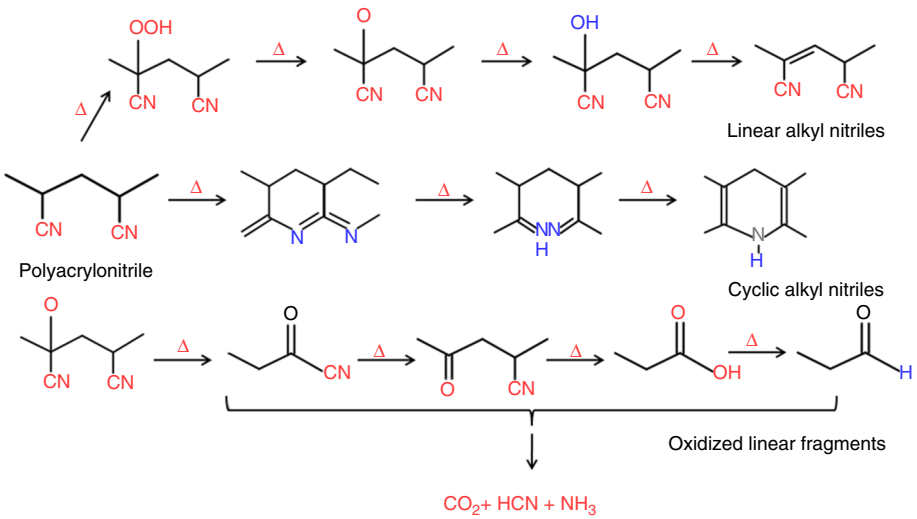

Table 6 IR bands of various peaks observed in the FTIR spectra of evolved gases

Heat treatment temperature/°C	Infrared group frequencies observed/cm^{-1}		Peak assignments
	A-PAC	I-PAC	
135	1 → 2935, 2 → 2848 3 → 1723, 4 → 1375 5 → 1081	1 → 2935, 2 → 2848 3a → 2240, 6 → 965 3, 4 and 5 disappear	1: N–H stretch; Alipahtic C–H stretch 2: C=N stretching; 3 → C–O stretch 3a: C=C(CN) 4: N–H stretching 5: C–N stretch, 6: C–C stretch
320	1 → 2935,2 → 2848 3 → 1723,4 → 1375 5 → 1081, 6 → 964 (appear)	1 → 2935, 2 → 2848 3 → Disappear; 4 → 1590 (appear), 5 → 1081; 6 → 964,7 → 714(appear)	1: N–H stretch; alipahtic C–H stretch 2: C=N stretching; 3: Alipahtic C–H bending 4: N–H stretching 5: C–N stretch 6: N–H (NH_3 release)
450	1 → 2935, 2 → 2848 3 → 1723, 4 → 1375 5 → 1081, 6 → 964 7 → 714, 8 → 3332	1 → 2935, 2 → 2848 3 → 1723, 4 → 1375 5 → 1081, 6 → 964 7 → 714, 8 → 3332	1: N–H stretch; alipahtic C–H stretch 2: C=N stretching; 3: Aliphatic C–O stretching 4: N–H stretching 5: C–N stretch 6. N–H (NH_3 release) 7: N–H bending (NH_3) 8: Aromatic—H stretch

Conclusions

In this work, two polyacrylonitrile copolymers differing in their stereoregularity (I-PAC (51.4%) A-PAC (48.8%) were synthesized; their average molecular masses, microstructure, and differential thermal behavior were investigated in detail, employing size-exclusion chromatography, solution viscometry, ^{13}C-NMR, and pyrolysis–gas chromatography–mass spectrometry (Py–GC–MS), evolved gas analysis–mass spectrometry (EGA–MS), and TG-FTIR, respectively. The volatile gaseous molecules evolved during the pyrolysis were obtained as total ion current thermal curves and pyrograms. Based on these results, four kinds of saturated and or unsaturated linear structures such as monomers, oligomers (dimers, trimers, and tetramers) accounting for the various homologous of linear alkyl nitriles were identified. An approximate fragmentation mechanism responsible for the release of evolved gases has been discussed. Fragmentation was related to the microstructural order in terms of triad tacticity content. The relatively more number and intensive peaks present in the pyrograms, mass, and FTIR spectra of A-PAC confirm that atactic-rich PAC are thermally more labile than I-PAC. Pyrolysis–GC–MS studies established that structural transformations and existence of different molecular species are due to thermal reactions, viz. α-cleavage, hydrogen-abstraction/elimination, and other thermal rearrangement reactions. Finally, an attempt has been made to identify the evolved gases released during the thermal decomposition and pyrolysis reactions of polyacrylonitrile co-polymeric materials closely resembling the carbon fiber fabrication process.

Acknowledgements Financial support by Council of Scientific and Industrial Research (CSIR), New Delhi, under Supra Institutional Project (SIP-IFCAP-04) is gratefully acknowledged. Authors are thankful to Tetsuro Yuzawa, Shiono, Frontier laboratories Ltd., Fukushima, Japan, for their thermal analysis support extended during this investigation. Authors thank the Director, CSIR-National Aerospace Laboratories, Bangalore, for his support and permission to publish this work.

References

1. Inui S. Present status and future of PAN based carbon fibre. In; Twenty-eighth seminar on composites, Japan carbon fibre manufacturers association, Tokyo, Japan, 2015; Feb 25.
2. Saito N, Aoki K, Usui Y, Shimizu M, Hara K, Narita K, Ogihara N, Nakamura K, Ishigaki N, Kato H, Haniu H, Taruta S, Kim YA. Endo M (2011) Application of carbon fibers to biomaterials: a new era of nano-level control of carbon fibers after 30-years of development. Chem Soc Rev. 2011;40:3824–34.

3. Frank O, Tsoukleri M, Papagelis RK, Parthenios J, Ferrari AC, Geim A, Novoselov KS, Galiotis C. Development of universal stress tensor for graphenes and carbon fibres. Nat Commun. 2011;2:255–61.
4. National historic chemical landmark programme, American Chemical Society, High performance carbon fibers, 2003; Sept 17.
5. Makoto E. Carbon fibre. Sen'I Gakkaishi (Fibre Ind). 2014;70:508–11.
6. Frank E, Steudle ML, Ingildeev D, Spcrl JM, Buckmeiser MR. Carbon fibers: precursor systems, processing, structure, and properties. Angew Chem Int Ed. 2014;53:5262–98.
7. Donnet JB, Bansal RC, editors. Carbon fibers. New York: Marcel Dekker Inc; 1998.
8. Arai Y. Pitch based carbon fiber. Tanso. 2010;241:15–21.
9. Long JW, Dunn B, Rolison DR, White HS. Three-dimensional battery architectures. Chem Rev. 2004;104:4463–92.
10. Committee on high-performance structural fibers for advanced composites. High-performance structural fibers for advanced polymer matrix composites. Washington: National Academic Press; 2005.
11. Daisuke K. Carbon fiber. Sen'I Gakkaishi. 2010;66:184.
12. Hiramatsu T. Tanso Sen'I no hon. Tokyo: Nikkan Publishers; 2012.
13. Hiromi A, Toru K. Polyacrylonitrile-based carbon fiber. Tanso. 2007;227:115.
14. Santhana Krishnan G. Pyrolysis and thermal stability of carbon fiber polymer precursors with different microstructures. In: Naskar AK, Hoffman WP, editors. Polymer derived carbon, ACS Sym Ser 1173. Washington: American Chemical Society; 2014. p. 169–87.
15. Fitzer E. Pan-based carbon fibers—present state and trend of the technology from the viewpoint of possibilities and limits to influence and to control the fiber properties by the process parameters. Carbon. 1989;2:621–45.
16. Usami T, Itoh T, Ohtani H, Tsuge S. Structural study of polyacrylonitrile fibers during oxidative thermal degradation by pyrolysis-gas chromatography, solid-state ^{13}C nuclear magnetic resonance, and fourier transform infrared spectroscopy. Macromolecules. 1990;23:2460–5.
17. Santhana Krishnan G, Thomas P, Murali N. Synthesis, characterization, and thermo mechanical properties of poly(acrylonitrile-co-2,3-dimethyl-1,3-butadiene-co-itaconic acid) as carbon fibre polymer precursors. RSC Adv. 2016;6:6182–90.
18. Gupta AK, Paliwal DK, Bajaj P. Effect of the nature and mole fraction of acidic comonomer on the stabilization of polyacrylonitrile. Macromol Sci Rev Macromol Chem Phys. 1991;1:301–10.
19. Yan X, Zhou W, Zhao X. Preparation, flame retardancy and thermal degradation behaviors of polyacrylonitrile fibers modified with diethylenetriamine and zinc ions. J Therm Anal Calorim. 2016;124:719–28.
20. Minnagawa M. An anomalous tacticity-crystallinity relationship: a WAXD study of stereoregular isotactic poly(acrylonitrile) powder prepared by urea clathrate polymerization. Macromolecules. 2001;34:3679–83.
21. Burkanudeen A, Santhana Krishnan G, Murali N. Thermal behavior of carbon fiber precursor polymers with different stereoregularities. J Therm Anal Calorim. 2013;112:1261–8.
22. Shimizu K. Recent progress in carbon fibers. Kobunshi. 1993;42(480–48):2.
23. Okamoto S, Ito A. Effects of nitrogen atoms on mechanical properties of graphenes by molecular dynamics simulations. Eng Lett. 2012;20:169–75.
24. Minnagawa M, Onuma H, Ogita T, Uchida H. Pyrolysis Gas chromatographic analysis of polyacrylonitril. J Appl Polym Sci. 2001;79:473–8.
25. Zhang WX, Liu J, Wu G. Evolution of structure and properties of PAN precursors during their conversion to carbon fibers. Carbon. 2003;41:2805–12.
26. Sumida A, Matsui J. Status and development of reinforcement fibres. Concr J. 1991;29(11):48–55.
27. Takuji S. Carbon fibres and their long term performance. J High Press Inst Jpn. 1997;35(3):125–32.
28. Santhana Krishnan G, Burkanudeen A, Murali N. Facile synthesis of stereoregular carbon fiber precursor polymers by template assisted solid phase polymerization. eXPRESS Polym Lett. 2012;6:729–73.
29. Tomoko I, Yuhei M. Method for producing polyacrylonitrile based fiber and method for producing carbon fiber. JP 2011-42893; 2011.
30. Sho T, Koichi S. Precursor for carbon fiber, method for producing the same. JP 2001-288613A; 2001.
31. Chuichi W. Development of analytical Py-GC system of polymericmaterials. Kobunshi. 1994;43:110–1.